

## SYNTHESIS, CHARACTERIZATION, ANTIMICROBIAL, ANTIOXIDANT ACTIVITIES, AND *IN SILICO* STUDY OF NEW AZO DISPERSE DYES CONTAINING PYRAZOLE AND PYRAZOLO[1,5-*A*]PYRIMIDINE RINGS

Mohamed I.H. El-Qaliei<sup>1\*</sup>, Sayed A.S. Mousa<sup>1</sup>, Esam A. Ishak<sup>1</sup>, Hamdi M.D. Nasr<sup>1</sup>, Modather F Hussein<sup>1,3</sup> and Abdallah M.A. Hassane<sup>2</sup>

<sup>1</sup>Chemistry Department, Faculty of Science, Al-Azhar University, Assiut 71524, Egypt

<sup>2</sup>Botany and Microbiology Department, Faculty of Science, Al-Azhar University, Assiut 71524, Egypt

<sup>3</sup>Chemistry Department, College of Science, Jouf University, PO Box 2014, Sakaka, Saudi Arabia

(Received December 6, 2024; Revised March 10, 2025; Accepted March 14, 2025)

**ABSTRACT.** New *N,N*-dimethyl-*N'*-(5-oxo-4-(aryldiazenyl)-2,5-dihydro-1*H*-pyrazol-3-yl)formimidamide **5a-c** are formed by reaction of 5-amino-1*H*-pyrazol-3(2*H*)-one derivatives **4a-c** with *N,N*-dimethylformamide dimethyl acetal (DMF-DMA). Compounds **5a-c** serve as excellent precursors for the synthesis of new disazo pyrazole disperse dyes. When refluxed with hydrazine hydrate or active methylene reagents **8a,b**, leading to *N'*-(3-hydroxy-4-(arylaza)-1*H*-pyrazol-5-yl)formimidohydrazide **7a-c** or pyrazolo[1,5-*a*]pyrimidines **11a-e**. *In vitro* studies were carried out to evaluate antioxidant properties of the produced compounds in comparison to standard, BHT. The results indicated that all the compounds exhibited varying levels of antioxidant activity at different doses. Compound (**7b**) exhibited an IC50 value comparable to that of BHT, while the other compounds demonstrated varying levels of activity and IC50 values in comparison to BHT. Regarding antimicrobial activity, compounds **7a**, **7b** and **11c** exhibited antibacterial efficiency against *Pseudomonas aeruginosa*, *Staphylococcus aureus*, and *Bacillus subtilis* with inhibition zone diameters of 14.33, 12.33, and 12.33 mm, respectively. *In silico* study of eleven pyrazole compounds with *S. aureus* 2XCT demonstrated strong hydrogen bonds, short distance interactions, and the highest binding energies were displayed by compounds **5b** and **11a** with binding energy of -6.6 and -6.2 kcal/mol, respectively.

**KEY WORDS:** Pyrazoles, DMFDMA, Antimicrobial, Antioxidant, Molecular docking, Disperse dyes, Pyrazolo[1,5-*a*]pyrimidines

### INTRODUCTION

Pyrazoles, five-membered heterocycles, are highly valuable in organic synthesis. They are among the most extensively studied compounds within the azole family. Over the years, numerous synthesis methods and synthetic analogues have been developed and documented. The incorporation of the pyrazole nucleus into various structures results in a wide range of applications across technology, medicine, and agriculture. Specifically, medical researchers are interested in the pyrazole structure because of its diverse variety of pharmacological effects; as antitubercular [1, 2], analgesic [3], anti-inflammatory [4, 5], antimicrobial [6-9], covid-19 main protease and papain-like protease inhibitors [10], antiviral [11,12], antidiabetic [13,14], carbonic anhydrase inhibitors [15] and glucosidase inhibitory activity [16]. Additionally, a variety of FDA-approved drugs contain the pyrazole pharmacophore, which is widely used in the pharmaceutical industry such as rimonabant [17], phenylbutazone [18], COX-II inhibitors [19], and anticancer drugs [20], anaesthetic effects, antibacterial, and fungicidal properties [21, 22], and against the Cotton Leafworm [23]. Pyrazolo [1,5-*a*]pyrimidines are analogues of purines with a wide range of biological applications, including inhibitors of acetylcholinesterase and amylase [24], sedative, antitrypanosomal and antimalarial agents [25], and selective inhibitors of COX-1 and COX-2

\*Corresponding authors. E-mail: mohamedahmed.136@azhar.edu.eg

This work is licensed under the Creative Commons Attribution 4.0 International License

[26]. Additionally, they are utilized in the therapy of a number of illnesses, including antifungal and antimalarial [27], antimicrobial [28], HIV reverse transcriptase [29], HCV inhibitors [30] and as KDR kinase inhibitors [31]. Commercially accessible medications containing pyrazolo[1,5-a]pyrimidine nucleus are included in [32-34].

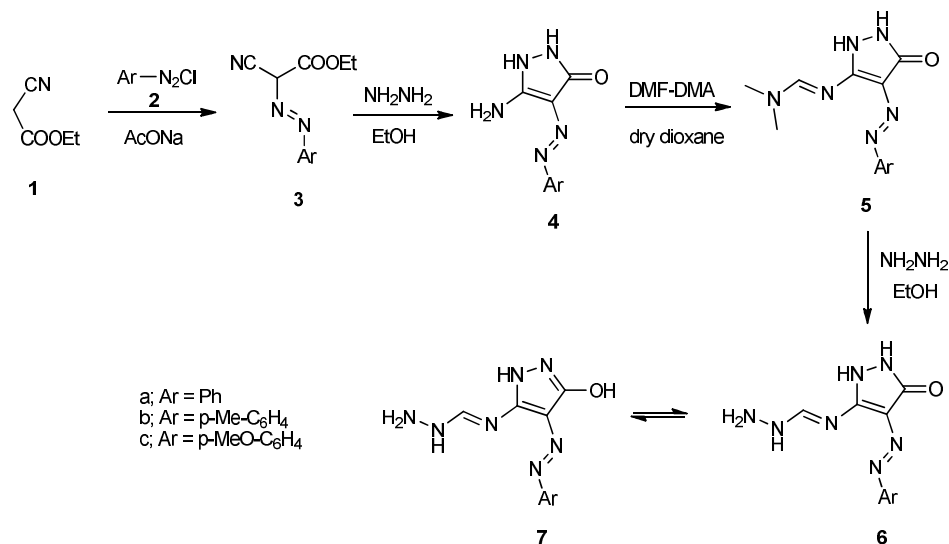
Evolution of chemical analytical techniques and computational tools has enabled the manufacture of antimicrobial compounds in drug discovery research [35] where structure-based drug design represents a crucial role [36]. Molecular docking provides a treasured tool for optimization and identification of drug candidates [37]. Molecular docking simulation is carried out to inspect the compounds' reliability of in protein-binding sites [37]. Integration of computational techniques enables rapid and cost-effective drug progress and suggesting new promises for diseases treating [38].

## RESULTS AND DISCUSSION

### Chemistry

The starting materials 5-amino-4-(aryldiazenyl)-1*H*-pyrazol-3(2*H*)-one **4a-c**, are shown in (Scheme 1) and were synthesized in accordance with previously published procedures [43].

Azo-aminopyrazole derivatives **4a-c** reacted with DMF-DMA (1:1) in refluxing dioxane to afford new imines **5a-c** (Scheme 1). Compound **5c** was selected as a sample example of the series produced to illustrate how the chemical structures of new compounds were confirmed *via* spectral data. The amino group band's disappearance from its IR spectrum and appearance of new signals at  $\delta_{\text{H}}$  3.09, 8.31, 10.54 and 11.04 ppm corresponding to  $\text{N}(\text{CH}_3)_2$ , (imine-H) and (exchangeable-2NH), respectively in its  $^1\text{H}$  NMR spectrum, in an addition of signals at  $\delta_{\text{C}}$  41.1, 55.9, 115.4, 117.3, 125.5, 148.8, 153.1, 156.8, 157.3, and 163.5 in its  $^{13}\text{C}$  NMR spectrum proved its structure.

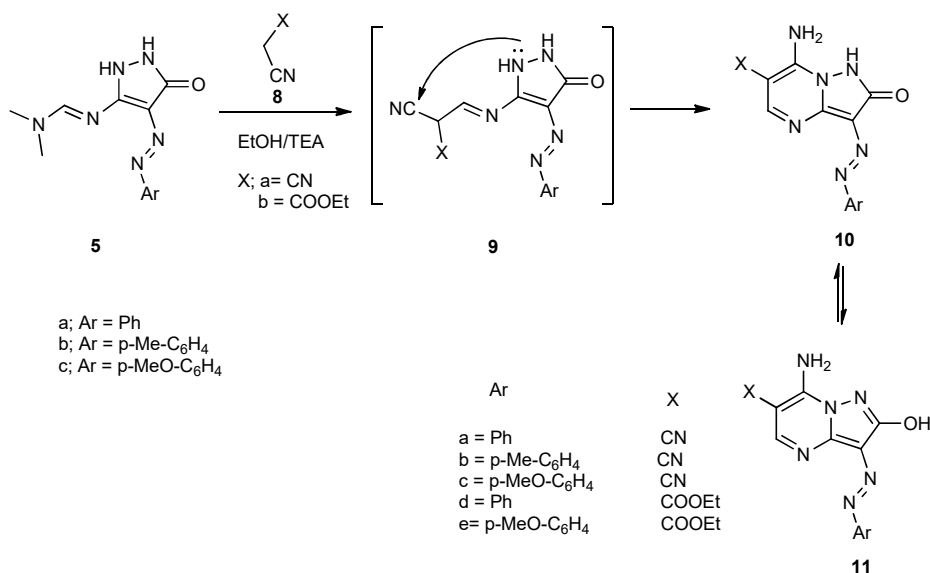


Scheme 1. Synthesis of imines **4a-c** - **7a-c**.

Imines **5a-c** are excellent starting materials to synthesize novel heterocyclic compounds through their reactions with nucleophilic reagents. Imines **5a-c** were allowed to react with hydrazine hydrate in refluxing ethanol to produce *N*'-(3-hydroxy-1*H*-pyrazol-5-

yl)formimidohydrazide **7a-c** (Scheme 1). IR spectrum of compound **7b** showed bands at 3396 and 3310 corresponding to hydroxyl and amino groups, while, its  $^1\text{H}$  NMR spectrum indicated signals at  $\delta_{\text{H}}$  5.77, 8.67, 9.08, 10.5 and 11.08 corresponding to (exchangeable- $\text{NH}_2$ ), (exchangeable-NH), (CH), (exchangeable-OH), and (exchangeable NH-pyrazole), respectively, While, its signals at  $\delta_{\text{C}}$  20.8, 120.7, 121.6, 128.5, 138.3, 146.0, 146.4, 148.6, and 160.0 were observed in the  $^{13}\text{C}$  NMR spectrum.

Finally, imines **5a-c** were reacted with active methylene compounds (malononitrile or ethyl cyanoacetate) **8a,b** in presence of triethylamine in ethanol to form new azo pyrazolo[1,5-a]pyrimidines **11a-e** (scheme 2). IR spectrum of compound **11c** showed absorption bands at 3405, 3312, and 2221  $\text{cm}^{-1}$  corresponding to hydroxyl, amino, and cyano groups, respectively. Its  $^1\text{H}$  NMR spectrum, appeared signals at  $\delta_{\text{H}}$  3.6, 8.49 and 8.93 corresponding to (exchangeable- $\text{NH}_2$ ), (pyrimidine-H) and (exchangeable-OH). Additionally, signals were detected in its  $^{13}\text{C}$  NMR spectrum at  $\delta_{\text{C}}$  56.0, 78.0, 115.0, 115.4, 116.0, 123.4, 144.7, 146.0, 149.1, 154.5, 160.5, and 161.1.



Scheme 2. Synthesis of azo pyrazolo[1,5-a]pyrimidines **5a-c**, **10a-e**, **11a-e**.

#### Antimicrobial activity

The antibacterial activity of test samples and reference standards (positive controls) was evaluated in vitro against a range of Gram-positive and Gram-negative bacterial strains, while *C. albicans* was subjected to antifungal assay. According to the results (Table, 1), compounds **7a,b** and **(11c)** showed antibacterial efficiency against *S. aureus*, *B. subtilis*, and *P. aeruginosa* with IZ diameters of 12.33, 12.33, and 14.33 mm, respectively. In general, the investigated compounds presented antibacterial activity showed fluctuated results in comparison to positive control. *C. albicans*, *K. pneumonia*, and *E. coli* had no susceptibility to any of the investigated compounds.

*Antioxidant activity*

Using the DPPH assay, the compounds' *in vitro* antioxidant properties were assessed by comparing them to the standard BHT (Table 2). All tested compounds exhibited varied antioxidant capacities at different concentrations as compared to standard. The IC<sub>50</sub> of compound (7b) showed homogeneity with BHT, whereas other examined compounds exhibited varying levels of activity and IC<sub>50</sub> in relation to BHT. Compounds 11b and 11c were not detected as their results were not applicable (Figure 1).

Table 1. Antimicrobial activity of the tested samples (5% w/v) against tested bacteria and *Candida* expressed using the well diffusion method as inhibitory diameter zones in mm.

Sample No.	<i>B. subtilis</i>	<i>S. aureus</i>	<i>E. coli</i>	<i>K. pneumonia</i>	<i>P. aeruginosa</i>	<i>C. albicans</i>
5a	ND	ND	ND	ND	ND	ND
5b	ND	ND	ND	ND	ND	ND
5c	ND	ND	ND	ND	ND	ND
7a	12.33±0.58 <sup>b</sup>	ND	ND	ND	ND	ND
7b	ND	ND	ND	ND	14.33±0.58 <sup>a</sup>	ND
7c	ND	ND	ND	ND	ND	ND
11a	ND	ND	ND	ND	ND	ND
11b	ND	ND	ND	ND	ND	ND
11c	ND	12.33±0.58 <sup>b</sup>	ND	ND	ND	ND
11d	ND	ND	ND	ND	ND	ND
11e	ND	ND	ND	ND	ND	ND
Chloramphenicol	16.33±0.58 <sup>a</sup>	15.67±0.58 <sup>a</sup>	14.33±0.58	14.67±0.58	14.67±0.58 <sup>a</sup>	-
Clotrimazole	-	-	-	-	-	18.67±0.58

The means of the data were displayed in triplicate (Mean±SD). The values represented by the different letters differ significantly at  $p < 0.05$ . - : Not tested; ND: Not detected.

Table 2. Antioxidant capacity and IC<sub>50</sub> value of the tested samples using DPPH assay.

Compound	Antioxidant capacity (%)					IC <sub>50</sub> value (mg extract/mL DPPH radicals)
	Conc. (mg/mL)					
	1	0.7	0.5	0.3	0.1	
5a	27.38±0.18	25.32±0.28	20.18±1.34	15.09±1.01	3.29±1.55	1.75
5b	36.27±0.59	29.94±0.89	25.21±0.45	22.21±0.34	3.41±0.53	1.33
5c	46.79±1.03	41.66±0.31	25.46±1.11	16.97±1.02	4.18±0.89	0.99
7a	63.57±0.32	59.73±0.05	51.20±0.23	45.31±0.96	41.40±0.68	0.44
7b	71.88±0.18	70.15±0.31	67.29±0.37	63.06±0.05	53.88±1.76	0.28
7c	64.25±1.12	58.87±0.77	52.25±1.16	47.23±0.34	35.44±0.51	0.47
11a	63.24±1.32	61.51±0.15	59.99±0.41	51.67±2.85	26.33±1.07	0.45
11b	ND	ND	ND	ND	ND	ND
11c	ND	ND	ND	ND	ND	ND
11d	19.60±0.18	17.29±0.65	13.71±0.49	11.25±0.72	6.63±0.72	3.06
11e	61.04±0.18	57.93±0.09	50.23±1.16	44.66±1.11	40.39±0.22	0.49
BHT	74.56±0.27	72.97±0.34	61.58±0.95	50.33±0.76	43.61±1.07	0.24

ND: not detected. Data were presented as means of triplicates (Mean±SD).

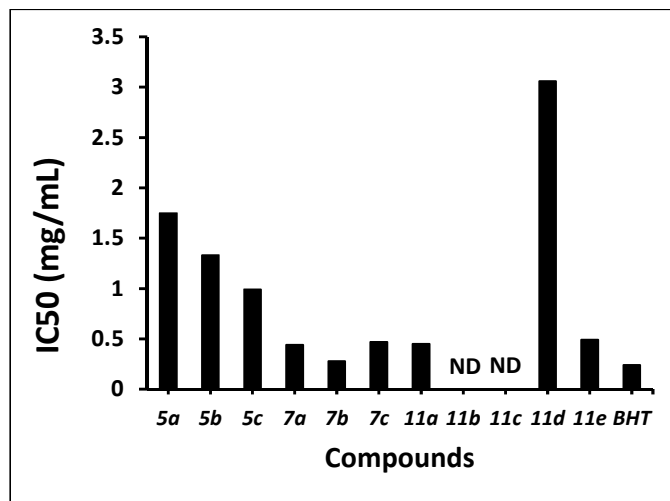


Figure 1. Antioxidant IC<sub>50</sub> values (mg/mL) of tested compounds.

#### Molecular docking simulation

The results of molecular docking simulations for 11 chemical compounds, testing their potential as antibacterial agents by interacting with the PDB structure of 2XCT was demonstrated. Strong hydrogen bonds, short distance interactions, and the highest binding energies were displayed by compounds **5b**, **11a**, and **11d**, while moderate binding energies and interactions were exhibited by compounds **7b**, **11c**, and **7c**. On the other hand, due to their weaker interactions and higher RMSD values, compounds **5a**, **7a**, and **11e** were less desirable.

Table 3. Docking pose score results of compounds interactions with targeted *S. aureus* topoisomerase IIA (2XRT).

Compound	S	RMSD (Å)	Ligand	Receptor	Interaction	Distance	Score (kcal/mol)
<b>5a</b>	-4.5296679	1.4984283	5-ring	CA LYS 581	pi-H	4.50	-1.0
<b>5b</b>	-5.0926318	1.7455839	N 12	NH2 ARG 1033	H-acceptor	2.75	-6.6
<b>5c</b>	-4.8278594	1.673272	O 8	NH1 ARG 1048	H-acceptor	2.65	-3.1
			N 9	NH2 ARG 1033	H-acceptor	2.79	-1.3
			C 31	5-ring HIS 1081	H-pi	3.74	-0.7
<b>7a</b>	-4.3773732	1.1774772	N 17	OD2 ASP 512	H-donor	3.40	-0.8
<b>7b</b>	-4.5751324	1.5075153	5-ring	CA ASP 1151	pi-H	4.57	-0.6
<b>7c</b>	-4.6434951	1.3758744	N 17	OD2 ASP 510	H-donor	3.24	-2.6
<b>11a</b>	-4.7583709	1.3688647	N 30	NH2 ARG 1048	H-acceptor	3.06	-6.2
<b>11b</b>	-4.7731805	1.677272	O 6	OD2 ASP 510	H-donor	2.94	-2.5
<b>11c</b>	-4.8030953	1.3484924	N 17	OD2 ASP 512	H-donor	3.39	-2.3
			6-ring	CA HIS 1081	pi-H	4.37	-0.7
<b>11d</b>	-5.525208	1.4983406	O 6	OD2 ASP 510	H-donor	2.97	-0.9
			6-ring	NE2 HIS 1081	pi-H	3.63	-1.6
<b>11e</b>	-4.9943485	1.8016832	6-ring	CB PRO 1080	pi-H	3.61	-0.6

Compound **5b** provided the strongest binding energy of -6.6 kcal/mol, thus indicated a potentially high affinity for the receptor 2XCT, making it a promising candidate for antibacterial activity. In addition, compound **11a** exhibited strong binding energy of -6.2 kcal/mol. In contrast, compound **7b** had a binding energy of -0.6 kcal/mol, indicating weaker binding, meanwhile compound **7a** displayed a binding energy of -0.8 kcal/mol, indicating weaker interaction with the receptor (Table 3).

Regarding types of interactions, several compounds formed hydrogen bonds with amino acid residues like ARG (e.g., **5b**, **5c**, and **11a**), ASP (e.g., **7a** and **11b**), and HIS (e.g., **11c** and **11d**). These interactions were typically strong and contributed significantly to the stability of the ligand-receptor complex. Many compounds (e.g., **5a**, **7b**, and **7c**) engaged in pi-H interactions, which could be crucial for the stability of the complex, especially in aromatic ring-based compounds. The distances between ligand atoms and receptor atoms ranged from 2.65 to 4.57 Å. Shorter distances (closer to 2.65 Å) generally indicated stronger interactions, with higher potential for binding. For instance, **5c** had interactions with ARG 1048 at a distance of 2.65 Å, suggesting a strong interaction (Figures 2-5). With their substantial binding energies and stable positions, compounds **5b** and **11d** are the best overall and are therefore excellent candidates for additional further research.

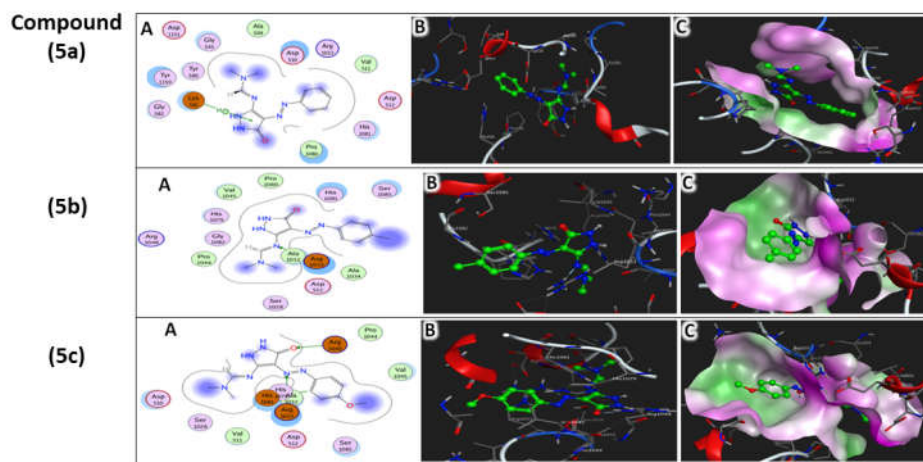


Figure 2. Two-D (A) and three-D (B and C) interactions diagrams of compounds (**5a**, **5b**, and **5c**) with 2XRT active site.

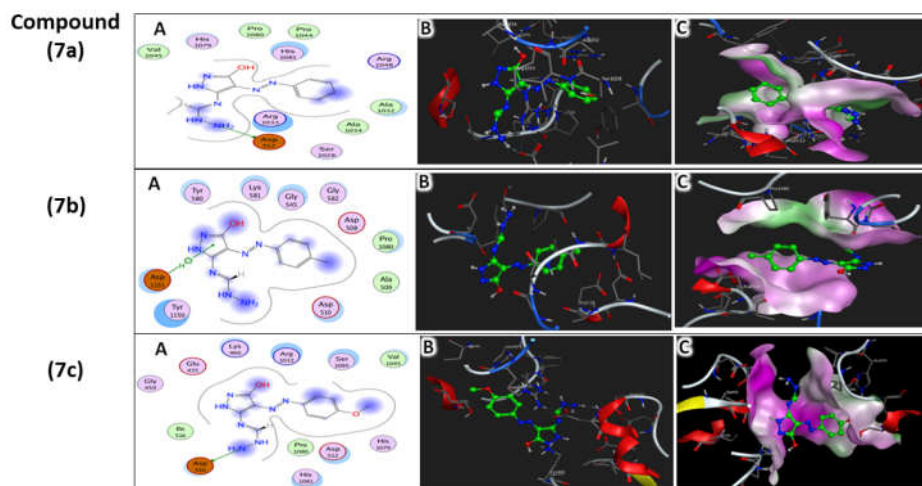


Figure 3. Two-D (A) and three-D (B and C) interactions diagrams of compounds (7a, 7b, and 7c) with 2XRT active site.

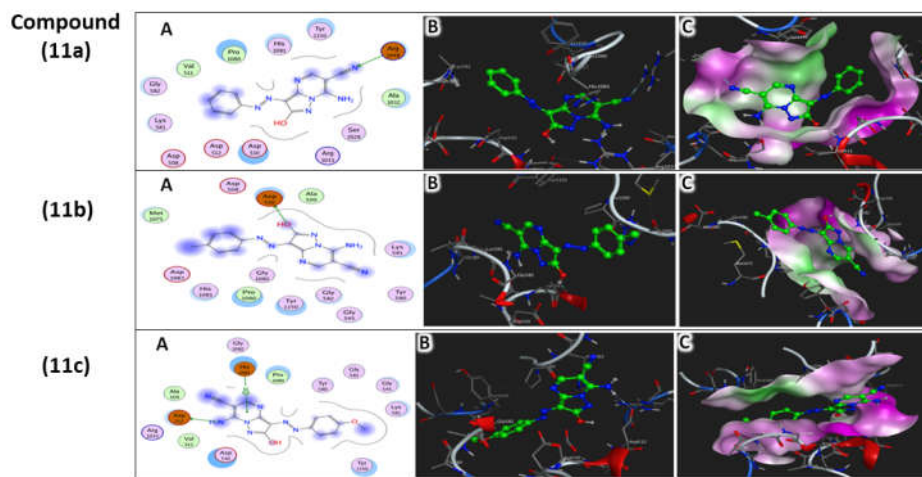


Figure 4. Two-D (A) and three-D (B and C) interactions diagrams of compounds (11a, 11b, and 11c) with 2XRT active site.

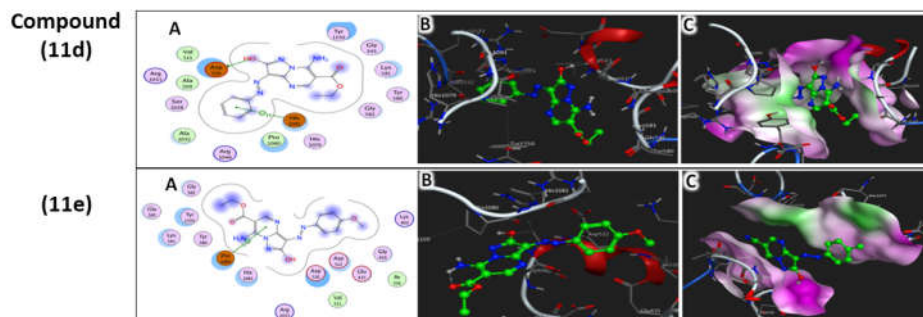


Figure 5. Two-D (A) and three-D (B and C) interactions diagrams of compounds (**11d** and **11e**) with 2XRT active site.

### EXPERIMENTAL

All melting points were measured on Kofler melting points equipment and are uncorrected. The IR spectra was obtained using a Nicolet 710 FT-IR spectrometer. On a Bruker A Vance III-400 MHz device,  $^1\text{H}$  NMR spectra are recorded at 400 MHz using  $\text{DMSO-}d_6$  as a solvent, while  $^{13}\text{C}$  NMR spectra are recorded at 100 MHz. Elemental microanalysis was performed using a Perkin-Elmer CHN-2400 elemental analyzer.

#### General method for synthesis of imines (**5a-c**)

A mixture of azo-aminopyrazole **4a-c** (0.01 mol) and DMF-DMA (1.32 mL, 0.01 mol) in dry dioxane (30 mL) was refluxed for 3 hours. The resultant solid was filtered off and recrystallized from ethanol.

*N,N*-Dimethyl-*N'*-[5-oxo-4-(*p*-phenyldiazenyl)-2,5-dihydro-1*H*-pyrazol-3-yl]formimidamide **5a**. Brown crystals; yield 77.5%; m.p. 162-164 °C; IR ( $\nu$ ,  $\text{cm}^{-1}$ ): 3440, 3196 (2NH) and 1696 (C=O);  $^1\text{H}$  NMR ( $\text{DMSO-}d_6$ , ppm): 3.11 (s, 6H,  $\text{N}(\text{CH}_3)_2$ ), 7.16-7.45 (m, 5H, aromatic-H), 8.34 (2s, 1H, imine-H), 10.62 and 11.12 (2s, 2H, exchangeable-2NH);  $^{13}\text{C}$  NMR: 40.6, 116.2, 123.7, 129.0, 129.1, 145.0, 149.6, 157.0 and 159.2. Anal. calc. for  $\text{C}_{12}\text{H}_{14}\text{N}_6\text{O}$ : C, 55.80; H, 5.46; N, 32.54. Found: C, 55.62; H, 5.34; N, 32.47.

*N,N*-Dimethyl-*N'*-5-oxo-4-(*p*-tolyl diazenyl)-2,5-dihydro-1*H*-pyrazol-3-yl formimidamide **5b**. Deep brown crystals; 81 % yield; m.p. 196-198 °C; IR ( $\nu$ ,  $\text{cm}^{-1}$ ): 3450, 3185 (2NH) and 1688(C=O);  $^1\text{H}$  NMR ( $\text{DMSO-}d_6$ , ppm): 2.3 (s, 3H,  $\text{CH}_3$ ), 2.98, 3.08 [2s, 6H,  $\text{N}(\text{CH}_3)_2$ ], 7.22, 7.34 (dd, 4H, aromatic-H), 8.39 (2s, 1H, imine-H), 10.58, 11.07 (2s, 2H, exchangeable-2NH);  $^{13}\text{C}$  NMR: 34.3, 41.4, 115.5, 116.4, 124.4, 148.3, 155.4, 156.4, 160.2 and 163.5. Anal. calc. for  $\text{C}_{13}\text{H}_{16}\text{N}_6\text{O}$ : C, 57.34; H, 5.92; N, 30.86. Found: C, 57.18; H, 5.72; N, 30.67.

*N'*-4-(*p*-Methoxyphenyl) diazenyl)-5-oxo-2,5-dihydro-1*H*-pyrazol-3-yl-*N,N*-dimethylformimidamide **5c**. Deep brown crystals; 85.7% yield; m.p. 182-184°C; IR ( $\nu$ ,  $\text{cm}^{-1}$ ): 3338, 3183 (2NH) and 1669 (C=O);  $^1\text{H}$  NMR ( $\text{DMSO-}d_6$ , ppm): 2.98, 3.09 [2s, 6H,  $\text{N}(\text{CH}_3)_2$ ], 3.78 (s, 3H,  $\text{OCH}_3$ ), 7.26, 7.42 (dd, 4H, aromatic-H), 8.31(2s, 1H, imine-H), 10.54 and 11.04 (2s, 2H, exchangeable-2NH);  $^{13}\text{C}$  NMR: 41.1, 55.9, 115.4, 117.3, 125.5, 148.8, 153.1, 156.8, 157.3, and 163.5. Anal. calc. for  $\text{C}_{13}\text{H}_{16}\text{N}_6\text{O}_2$ : C, 54.16; H, 5.59; N, 29.15. Found: C, 53.95; H, 5.39; N, 28.94.



*General method for synthesis of compounds 7a-c*

A mixture of imines **5a-c** (0.01 mol) and hydrazine hydrate (0.015 mol) in ethanol was refluxed for 4 hours. The resultant solid was filtered off and recrystallized from ethanol.

*N''*-(3-Hydroxy-4-(*p*-phenyldiazenyl)-1*H*-pyrazol-5-yl)formimidohydrazide **7a**. Brownish yellow crystals; 73.4% yield; m.p. 215-217 °C; IR ( $\nu$ ,  $\text{cm}^{-1}$ ): 3404 (OH), 3334 ( $\text{NH}_2$ ), 3205 and 3151 (2NH);  $^1\text{H}$  NMR (DMSO- $d_6$ , ppm): 5.86 (d, 2H, exchangeable- $\text{NH}_2$ ), 7.19-7.68 (m, 5H, aromatic-H), 8.7(d, 1H, exchangeable-NH), 9.13(d, 1H, imine-H), 10.56(s, 1H, exchangeable-OH), 11.14(s, 1H, NH);  $^{13}\text{C}$  NMR: 120.8, 122.2, 128.9, 129.0, 146.4, 148.7, 161.4. Anal. calc. for  $\text{C}_{10}\text{H}_{11}\text{N}_7\text{O}$ : C, 48.98; H, 4.52; N, 39.98. Found: C, 48.79; H, 4.46; N, 39.82.

*N''*-(3-Hydroxy-4-(*p*-tolyl diazenyl)-1*H*-pyrazol-5-yl)formimidohydrazide **7b**. Orange crystals; 77.2% yield; m.p. 230-232 °C; IR ( $\nu$ ,  $\text{cm}^{-1}$ ): 3396 (OH), 3310 ( $\text{NH}_2$ ), 3246 and 3222 (2NH);  $^1\text{H}$  NMR (DMSO- $d_6$ , ppm): 2.33 (s, 1H,  $\text{CH}_3$ ), 5.77 (d, 2H, exchangeable- $\text{NH}_2$ ), 7.26, 7.43(dd, 4H, aromatic-H), 8.67 (d, 1H, exchangeable-NH), 9.08 (d, 1H, imine-H), 10.5 (s, 1H, exchangeable-OH), 11.08 (s, 1H, NH);  $^{13}\text{C}$  NMR: 20.8, 120.7, 121.6, 128.5, 138.3, 146.0, 146.4, 148.6 and 160.0. Anal. calc. for  $\text{C}_{11}\text{H}_{13}\text{N}_7\text{O}$ : C, 50.96; H, 5.05; N, 37.82. Found: C, 50.82; H, 5.14; N, 37.72.

*N''*-(3-Hydroxy-4-(4-methoxyphenyl) diazenyl)-1*H*-pyrazol-5-yl)formimidohydrazide **7c**. Orange crystals; 76.4% yield; m.p. 200-202 °C; IR ( $\nu$ ,  $\text{cm}^{-1}$ ): 3423 (OH), 3332 ( $\text{NH}_2$ ), 3211 and 3178 (2NH);  $^1\text{H}$  NMR (DMSO- $d_6$ , ppm): 3.79 (s, 1H,  $\text{OCH}_3$ ), 5.77 (d, 2H, exchangeable- $\text{NH}_2$ ), 7.03, 7.63(dd, 4H, aromatic-H), 8.61 (d, 1H, exchangeable-NH), 9.05 (d, 1H, imine-H), 10.49 (s, 1H, exchangeable-OH), 11.06 (s, 1H, NH);  $^{13}\text{C}$  NMR: 55.4, 114.2, 121.0, 121.8, 146.0, 146.4, 147.8, 158.3 and 159.9. Anal. calc. for  $\text{C}_{11}\text{H}_{13}\text{N}_7\text{O}_2$ : C, 48.00; H, 4.76; N, 35.62. Found: C, 47.2; H, 4.65; N, 35.49.

*General method for synthesis of pyrazolo[1,5-*a*]pyrimidines 11a-e*

A mixture of imines **5a-c** (0.01 mol) and active methylene compounds **8a,b** (0.01 mol) in ethanol with a few drops of triethylamine was refluxed for 6 hours. The resultant solid was filtered off and recrystallized from DMF and ethanol mixture (1:3).

7-Amino-2-hydroxy-3-(*p*-phenyldiazenyl)pyrazolo[1,5-*a*]pyrimidine-6-carbonitrile **11a**. Brown crystals; 75.2% yield; m.p. 285-287 °C; IR ( $\nu$ ,  $\text{cm}^{-1}$ ): 3382 (OH), 3324 ( $\text{NH}_2$ ) and 2223 ( $\text{C}\equiv\text{N}$ );  $^1\text{H}$  NMR (DMSO- $d_6$ , ppm): 5.86 (s, 2H, exchangeable- $\text{NH}_2$ ), 7.11-7.84(m, 5H, aromatic-H), 8.53(s, 1H, pyrimidine-H) and 10.56 (s, 1H, exchangeable-OH);  $^{13}\text{C}$  NMR: 108.6, 115.0, 121.6, 122.4, 129.2, 129.6, 145.6, 147.0, 150.2, 154.1 and 157.0. Anal. calc. for  $\text{C}_{13}\text{H}_9\text{N}_7\text{O}$ : C, 55.91; H, 3.25; N, 35.11. Found: C, 55.79; H, 3.09; N, 35.15.

7-Amino-2-hydroxy-3-(*p*-tolyl diazenyl)pyrazolo[1,5-*a*]pyrimidine-6-carbonitrile **11b**. Red brown crystals; 78.5% yield; m.p. 298-300 °C; IR ( $\nu$ ,  $\text{cm}^{-1}$ ): 3357 (OH), 3313 ( $\text{NH}_2$ ) and 2225 ( $\text{C}\equiv\text{N}$ );  $^1\text{H}$  NMR (DMSO- $d_6$ , ppm): 2.38(s,3H,  $\text{CH}_3$ ), 4.24 (br, 2H, exchangeable- $\text{NH}_2$ ), 7.33, 7.73(2d, 4H, aromatic-H), 8.51(s, 1H, pyrimidine-H) and 8.89 (br, 1H, exchangeable-OH);  $^{13}\text{C}$  NMR: 21.1, 108.6, 115.0, 119.8, 121.7, 129.0, 138.9, 145.7, 146.8, 148.4, 154.0 and 157.4. Anal. calc. for  $\text{C}_{14}\text{H}_{11}\text{N}_7\text{O}$ : C, 57.33; H, 3.78; N, 33.43. Found: C, 57.24; H, 3.64; N, 33.12.

7-Amino-3-(4-methoxyphenyl) diazenyl-2-oxo-1,2-dihydropyrazolo[1,5-*a*]pyrimidine-6-carbonitrile **11c**. Brown crystals; 77.6% yield; m.p. over 300 °C; IR ( $\nu$ ,  $\text{cm}^{-1}$ ): 3405 (OH), 3312 ( $\text{NH}_2$ ) and 2221 ( $\text{C}\equiv\text{N}$ );  $^1\text{H}$  NMR (DMSO- $d_6$ , ppm):  $\delta$  3.6(br, 2H, exchangeable- $\text{NH}_2$ ), 3.85 (s, 3H,  $\text{OCH}_3$ ), 7.09, 7.85 (dd, 4H, aromatic-H), 8.49(s, 1H, pyrimidine-H) and 8.93 (br, 1H,

exchangeable-OH);  $^{13}\text{C}$  NMR: 56.0, 78.0, 115.0, 115.4, 116.0, 123.4, 144.7, 146.0, 149.1, 154.5, 160.5 and 161.1. Anal. calc. for  $\text{C}_{14}\text{H}_{11}\text{N}_7\text{O}_2$ : C, 54.37; H, 3.58; N, 31.70. Found: C, 54.21; H, 3.42; N, 31.56.

*Ethyl-7-amino-2-hydroxy-3-(phenyldiazenyl)pyrazolo[1,5-a]pyrimidine-6-carboxylate* **11d**. Brownish yellow crystals; 76.7% yield; m.p. 278-280 °C; IR ( $\nu$ ,  $\text{cm}^{-1}$ ): 3399 (OH), 3324 ( $\text{NH}_2$ ) and 1697 (C=O);  $^1\text{H}$  NMR (DMSO- $d_6$ , ppm): 1.37 (t, 3H,  $\text{CH}_3$ ), 4.39 (q, 2H,  $\text{CH}_2$ ), 5.86 (s, 2H, exchangeable- $\text{NH}_2$ ), 7.15-7.84 (m, 5H, aromatic-H), 8.33 (s, 1H, pyrimidine-H) and 10.62 (s, 1H, exchangeable-OH);  $^{13}\text{C}$  NMR: 14.4, 59.6, 109.3, 122.6, 125.0, 129.1, 130.0, 145.9, 146.7, 149.5, 152.0, 157.5 and 164.3. Anal. calc. for  $\text{C}_{15}\text{H}_{14}\text{N}_6\text{O}_3$ : C, 55.21; H, 4.32; N, 25.75. Found: C, 55.12; H, 4.17; N, 25.59.

*Ethyl-7-amino-2-hydroxy-3-(4-methoxyphenyl)diazenylpyrazolo[1,5-a]pyrimidine-6-carboxylate* **11e**. Red brown crystals; 73 % yield; m.p. 260-262 °C; IR ( $\nu$ ,  $\text{cm}^{-1}$ ): 3403 (OH), 3328 ( $\text{NH}_2$ ) and 1685 (C=O);  $^1\text{H}$  NMR (DMSO- $d_6$ , ppm):  $\delta$  1.37 (t, 3H,  $\text{CH}_3$ ), 4.36 (q, 2H,  $\text{CH}_2$ ), 5.77 (s, 2H, exchangeable- $\text{NH}_2$ ), 7.03, 7.52 (dd, 4H, aromatic), 8.32 (s, 1H, pyrimidine-H) and 11.03 (s, 1H, exchangeable-OH);  $^{13}\text{C}$  NMR: 14.7, 55.5, 59.8, 109.3, 114.3, 123.3, 125.1, 144.4, 146.7, 150.2, 153.0, 154.8, 159.0 and 164.5. Anal. calc. for  $\text{C}_{16}\text{H}_{16}\text{N}_6\text{O}_4$ : C, 53.93; H, 4.53; N, 23.58. Found: C, 53.78; H, 4.39; N, 23.42.

#### Evaluating antimicrobial activities

Pathogenic strains of *Pseudomonas aeruginosa* ATCC 9027, *Klebsiella pneumonia* ATCC 43816, *Escherichia coli* ATCC 8739, *Bacillus subtilis* ATCC 6633, and *Staphylococcus aureus* ATCC 6538, in addition to one fungal strain, *Candida albicans* ATCC 10231, were used previously by [40] as test microbes for biological activities assessment. Muller-Hinton and Sabouraud dextrose media, inoculated previously with cultures of the test strains, were used for assessing antibacterial and antifungal activities, respectively. Agar well diffusion method was performed as described by [41] with 8 mm diameter hole that is filled with 100  $\mu\text{L}$  of 5% (w/v) investigated compounds dispersed by sonication in dimethyl sulfoxide. Chloramphenicol and clotrimazole, at concentrations of 1 mg/mL, were utilized as positive controls for bacteria and *C. albicans*, respectively. Positive bioactivity was indicated by measuring the inhibitory zone's diameter (IZ) in millimetres.

#### DPPH radical scavenging activity

The antioxidant capacity of test compounds was evaluated by DPPH radical scavenging assay [42]. 1.8 mL of 0.1 mM DPPH solution was added to 0.2 ml of the test sample at different concentrations (1, 0.7, 0.5, 0.3 and 0.1 mg/mL). After being left at room temperature for half an hour, the absorbance at 517 nm was measured using a spectrophotometer. Butylated hydroxytoluene (BHT) was utilized as the positive control, while negative control was represented by positive control. The following formula was used to determine the DPPH radical's scavenging capacity:

$$\% \text{ DPPH radical scavenging} = \frac{A - B}{A} \times 100 \quad (1)$$

where A represents the absorbance of the negative control and B denotes the sample's absorbance. The regression equation ( $y = ax + b$ ) was used to determine the  $\text{IC}_{50}$ , and the resulting estimate was  $\text{IC}_{50} = (0.5 - b)/a$ .

*Statistical analysis*

Every test was run three times; averages were established by analysis of variance (ANOVA) using SPSS, program version 16, and statistical analysis was conducted (at  $p < 0.05$ ).

*Molecular docking simulation*

The docking analysis was performed by assessing the inhibition of *S. aureus* topoisomerase IIA (pdb code 2XRT) using Autodock package [43]. The docked ligands of *S. aureus* topoisomerase IIA was obtained from the RCSB Protein Data Bank (<http://www.rcsb.org/pdb> (accessed on 20 June 2024)). The protein active target was selected and as the complex inhibitor ligand site. Further, 11 tested compounds were vindicated, and generation of a virtual ligand database was carried out. The docking scores were documented by a firm receptor-flexible ligand-docking method, while 2D and 3D interaction figures were constructed using MOE 2015.

**CONCLUSION**

Utility of azo aminopyrazole as precursors to synthesize new imines, *N*'-(3-hydroxy-1*H*-pyrazol-5-yl)formimidohydrazide and azo pyrazolo[1,5-*a*] pyrimidines by refluxed with (DMF-DMA), hydrazine hydrate and active methylene reagents. The antibacterial and antioxidant properties of recently synthesized substances are assessed. To identify potential bacterial targets, an in-silico study was initiated. Molecular docking simulations for eleven chemical compounds with the PDB structure of 2XCT demonstrated strong hydrogen bonds, short distance interactions, and the highest binding energies were displayed by compounds **5b** and **11a** representing valuable candidates for further research.

**REFERENCES**

1. Meta, E.; Brullo, C.; Tonelli, M.; Franzblau, S.G.; Wang, Y.; Ma, R.; Baojie, W.; Orena, B.S.; Pasca, M.R.; Bruno, O. Pyrazole and imidazo [1, 2-*b*] pyrazole derivatives as new potential anti-tuberculosis agents. *Med. Chem. (Los Angeles)*. **2019**, 15, 17-27.
2. Xu, Z.; Gao, C.; Ren, Q.-C.; Song, X.-F.; Feng, L.-S.; Lv, Z.-S. Recent advances of pyrazole-containing derivatives as anti-tubercular agents. *Eur. J. Med. Chem.* **2017**, 139, 429-440.
3. Khalifa, N.M.; Fahmy, H.H.; Nossier, E.S.; Amr, A.E.G.E.; Herqash, R.N. Novel synthesis of pyrazole-containing thiophene, 2-alkyloxy-pyridine and thieno [2, 3-*d*] pyrimidine scaffolds as analgesic agents. *Bull. Chem. Soc. Ethiop.* **2019**, 33, 505-515.
4. Engers, D.W.; Frist, A.Y.; Lindsley, C.W.; Hong, C.C.; Hopkins, C.R. Synthesis and Structure-activity relationships of a novel and selective bone morphogenetic protein receptor (BMP) inhibitor derived from the pyrazolo [1.5-*a*] pyrimidine scaffold of dorsomorphin: The discovery of ML347 as an ALK2 versus ALK3 selective MLPC. *Bioorg. Med. Chem. Lett.* **2013**, 23, 3248-3252.
5. Ayman, R.; Radwan, A.M.; Elmetwally, A.M.; Ammar, Y.A.; Ragab, A. Discovery of Novel pyrazole and pyrazolo [1, 5-*a*] pyrimidine derivatives as cyclooxygenase inhibitors (COX-1 and COX-2) using molecular modeling simulation. *Arch. Pharm. (Weinheim)*. **2023**, 356, 2200395.
6. Mohamed, H.A.; Ammar, Y.A.; Elhagali, G.A.M; Eyada, H.A.; Aboul-Magd, D.S.; Ragab, A. In vitro antimicrobial evaluation, single-point resistance study, and radiosterilization of novel pyrazole incorporating thiazol-4-one/thiophene derivatives as dual DNA Gyrase and DHFR inhibitors against MDR pathogens. *ACS Omega* **2022**, 7, 4970-4990.

7. El-Qaliei, M.I.H.; Mousa, S.A.S.; Nasr, H.M.D.; İshak, E.A. 5-Amino-3-(cyanomethyl)-1h-pyrazole-4-carbonitrile as precursor for synthesis of some novel pyrazolo [1, 5-a] pyrimidine derivatives. *Egypt. J. Chem.* **2022**, *65*, DOI: 10.21608/ejchem.2022.124950.5560.
8. Nour Eldeen, F.B.; Mousa, S.A.S.; Othman, I.M.M.; El-Qaliei, M.I.H. New Pyrazolo [1, 5-a] pyrimidine, pyrimido [1', 2': 1, 5] pyrazolo [3, 4-d] pyridazine and its fused derivatives: Synthesis, characterization and antimicrobial evaluation. *Egypt. J. Chem.* **2023**, *66*, 2269-2278.
9. Eldeen, F.B.N.; Mousa, S.A.S.; Othman, I.M.M.; El-Qaliei, M.I.H. Design, synthesis, antimicrobial evaluation, molecular docking studies, and in silico prediction of adme properties for novel pyrazolo [1, 5-a] pyrimidine and its fused derivatives. *J. Heterocycl. Chem.* **2024**, *61*, DOI:10.1002/jhet.4814.
10. Khatab, T.K.; Hassan, A. S. Computational molecular docking and in silico ADMET prediction studies of pyrazole derivatives as COVID-19 main protease (Mpro) and papain-like protease (PLpro) inhibitors. *Bull. Chem. Soc. Ethiop.* **2023**, *37*, 449-461.
11. Da Costa, L.; Scheers, E.; Coluccia, A.; Casulli, A.; Roche, M.; Di Giorgio, C.; Neyts, J.; Terme, T.; Cirilli, R.; La Regina, G. Structure-based drug design of potent pyrazole derivatives against rhinovirus replication. *J. Med. Chem.* **2018**, *61*, 8402-8416.
12. Al-Zharani, M.; Al-Eissa, M.S.; Rudayni, H.A.; Ali, D.; Alkahtani, S.; Surendrakumar, R.; Idhayadhulla, A. Pyrazolo [3, 4-b] pyridin-3 (2h)-one derivatives: Synthesis and their investigation of mosquito larvicidal activity. *J. King Saud Univ.* **2022**, *34*, 101767.
13. Naim, M.J.; Alam, O.; Alam, M.J.; Hassan, M.Q.; Siddiqui, N.; Naidu, V.G.M.; Alam, M.I. Design, synthesis and molecular docking of thiazolidinedione based benzene sulphonamide derivatives containing pyrazole core as potential anti-diabetic agents. *Bioorg. Chem.* **2018**, *76*, 98-112.
14. Faidallah, H.M.; Al-Mohammadi, M.M.; Alamry, K.A.; Khan, K.A. Synthesis and biological evaluation of fluoropyrazolesulfonylurea and thiourea derivatives as possible antidiabetic agents. *J. Enzyme Inhib. Med. Chem.* **2016**, *31*, 157-163.
15. Wassel, M.M.S.; Ragab, A.; Ali, G.A.M.E.; Mehany, A.B.M.; Ammar, Y.A. Novel adamantane-pyrazole and hydrazone hybridized: design, synthesis, cytotoxic evaluation, SAR study and molecular docking simulation as carbonic anhydrase inhibitors. *J. Mol. Struct.* **2021**, *1223*, 128966.
16. Chaudhry, F.; Naureen, S.; Choudhry, S.; Huma, R.; Ashraf, M.; Al-Rashida, M.; Jahan, B.; Khan, M.H.; Iqbal, F.; Munawar, M.A. Evaluation of  $\alpha$ -glucosidase inhibiting potentials with docking calculations of synthesized arylidene-pyrazolones. *Bioorg. Chem.* **2018**, *77*, 507-514.
17. Ortega, J.E.; Gonzalez-Lira, V.; Horrillo, I.; Herrera-Marschitz, M.; Callado, L.F.; Meana, J.J. Additive effect of rimonabant and citalopram on extracellular serotonin levels monitored with in vivo microdialysis in rat brain. *Eur. J. Pharmacol.* **2013**, *709*, 13-19.
18. De Grauw, J.C.; Van Loon, J.; Van de Lest, C.H.A.; Brunott, A.; Van Weeren, P.R. In vivo effects of phenylbutazone on inflammation and cartilage-derived biomarkers in equine joints with acute synovitis. *Vet. J.* **2014**, *201*, 51-56.
19. Fioravanti, R.; Bolasco, A.; Manna, F.; Rossi, F.; Orallo, F.; Ortuso, F.; Alcaro, S.; Cirilli, R. Synthesis and biological evaluation of n-substituted-3, 5-diphenyl-2-pyrazoline derivatives as cyclooxygenase (COX-2) inhibitors. *Eur. J. Med. Chem.* **2010**, *45*, 6135-6138.
20. Devi, N.; Shankar, R.; Singh, V. 4-Formyl-pyrazole-3-carboxylate: A useful aldo-X bifunctional precursor for the syntheses of pyrazole-fused/substituted frameworks. *J. Heterocycl. Chem.* **2018**, *55*, 373-390.
21. El-Qaliei, M.I.H.; Mousa, S.A.S.; Mahross, M.H.; Hassane, A.M.A.; Gad-Elkareem, M.A.M.; Snoussi, M.; Aouadi, K.; Kadri, A. Novel (2-oxindolin-3-ylidene) methyl)-1h-pyrazole and their fused derivatives: Design, synthesis, antimicrobial evaluation, DFT, chemical approach, in silico ADME and molecular docking studies. *J. Mol. Struct.* **2022**, *1264*, 133299.

22. Khokhlova, O.N.; Borozdina, N.A.; Sadovnikova, E.S.; Pakhomova, I.A.; Rudenko, P. A.; Korolkova, Y.V.; Kozlov, S.A.; Dyachenko, I.A. Comparative study of the aftereffect of CO<sub>2</sub> inhalation or tiletamine–zolazepam–xylazine anesthesia on laboratory outbred rats and mice. *Biomedicines* **2022**, *10*, 512.
23. Mousa, S.A.S.; El-Qalici, M.I.H.; Atalla, A.A.; Hussien, A.H.H.; Khodairy, A.; Abdou, A.; Drar, A.M.; Gad, M.A. Synthesis, insecticide evaluation & molecular docking studies of some new functionalized pyrazole derivatives against the cotton leafworm, *spodoptera littoralis*. *Chem. Biodivers.* **2024**, *21*, e202400831.
24. Hassan, A.S.; Morsy, N.M.; Aboulthana, W.M.; Ragab, A. In vitro enzymatic evaluation of some pyrazolo [1, 5-*a*] pyrimidine derivatives: design, synthesis, antioxidant, anti-diabetic, anti-alzheimer, and anti-arthritis activities with molecular modeling simulation. *Drug Dev. Res.* **2023**, *84*, 3-24.
25. Abdelgawad, M.A.; Elkanzi, N.A.A.; Musa, A.; Ghoneim, M.M.; Ahmad, W.; Elmowafy, M.; Ali, A.M.A.; Abdelazeem, A.H.; Bukhari, S.N.A.; El-Sherbiny, M. Optimization of pyrazolo [1, 5-*a*] pyrimidine based compounds with pyridine scaffold: Synthesis, Biological evaluation and molecular modeling study. *Arab. J. Chem.* **2022**, *15*, 104015.
26. Fraley, M.E.; Rubino, R.S.; Hoffman, W.F.; Hambaugh, S.R.; Arrington, K.L.; Hungate, R.W.; Bilodeau, M.T.; Tebben, A.J.; Rutledge, R.Z.; Kendall, R.L. Optimization of a pyrazolo [1, 5-*a*] pyrimidine class of kdr kinase inhibitors: Improvements in physical properties enhance cellular activity and pharmacokinetics. *Bioorg. Med. Chem. Lett.* **2002**, *12*, 3537-3541.
27. Ivachtchenko, A.V.; Dmitriev, D.E.; Golovina, E.S.; Kadieva, M.G.; Koryakova, A.G.; Kysil, V.M.; Mitkin, O.D.; Okun, I.M.; Tkachenko, S.E.; Vorobiev, A.A. (3-Phenylsulfonylcycloalkano [e and d] pyrazolo [1, 5-*a*] pyrimidin-2-yl) amines: Potent and selective antagonists of the serotonin 5-HT<sub>6</sub> receptor. *J. Med. Chem.* **2010**, *53*, 5186-5196.
28. Hassan, A.S.; Morsy, N.M.; Awad, H.M.; Ragab, A. Synthesis, molecular docking, and in silico ADME prediction of some fused pyrazolo [1, 5-*a*] pyrimidine and pyrazole derivatives as potential antimicrobial agents. *J. Iran. Chem. Soc.* **2022**, *19*, 521-545.
29. Hwang, J.Y.; Windisch, M.P.; Jo, S.; Kim, K.; Kong, S.; Kim, H.C.; Kim, S.; Kim, H.; Lee, M.E.; Kim, Y. Discovery and characterization of a novel 7-aminopyrazolo [1, 5-*a*] pyrimidine analog as a potent hepatitis C virus inhibitor. *Bioorg. Med. Chem. Lett.* **2012**, *22*, 7297-7301.
30. Selli, S.; Bruni, F.; Costagli, C.; Costanzo, A.; Guerrini, G.; Ciciani, G.; Costa, B.; Martini, C. 2-Arylpyrazolo [1, 5-*a*] pyrimidin-3-yl acetamides. new potent and selective peripheral benzodiazepine receptor ligands. *Bioorg. Med. Chem.* **2001**, *9*, 2661-2671.
31. Selli, S.; Bruni, F.; Costagli, C.; Costanzo, A.; Guerrini, G.; Ciciani, G.; Gratteri, P.; Besnard, F.; Costa, B.; Montali, M. A novel selective GABAA A1 Receptor agonist displaying sedative and anxiolytic-like properties in rodents. *J. Med. Chem.* **2005**, *48*, 6756-6760.
32. Asati, V.; Anant, A.; Patel, P.; Kaur, K.; Gupta, G.D. Pyrazolopyrimidines as anticancer agents: A review on structural and target-based approaches. *Eur. J. Med. Chem.* **2021**, *225*, 113781.
33. Cherukupalli, S.; Hampannavar, G.A.; Chinnam, S.; Chandrasekaran, B.; Sayyad, N.; Kayamba, F.; Aleti, R.R.; Karpoornath, R. An appraisal on synthetic and pharmaceutical perspectives of pyrazolo [4, 3-*d*] pyrimidine scaffold. *Bioorg. Med. Chem.* **2018**, *26*, 309-339.
34. Cherukupalli, S.; Karpoornath, R.; Chandrasekaran, B.; Hampannavar, G.A.; Thapliyal, N.; Palakollu, V.N. An insight on synthetic and medicinal aspects of pyrazolo [1, 5-*a*] pyrimidine scaffold. *Eur. J. Med. Chem.* **2017**, *126*, 298-352.
35. Al Mousa, A.A.; Abouelela, M.E.; Al Ghamidi, N.S.; Abo-Dahab, Y.; Mohamed, H.; Abo-Dahab, N.F.; Hassane, A.M.A. Anti-staphylococcal, anti-candida, and free-radical scavenging potential of soil fungal metabolites: A study supported by phenolic characterization and molecular docking analysis. *Curr. Issues Mol. Biol.* **2023**, *46*, 221-243.

36. Chopade, A.R.; Sayyad, F.J.; Pore, Y.V. Molecular docking studies of phytochemicals from the phyllanthus species as potential chronic pain modulators. *Sci. Pharm.* **2014**, *83*, 243.
37. Othman, I.M.M.; Gad-Elkareem, M.A.M.; Aouadi, K.; Snoussi, M.; Kadri, A. New substituted pyrazolones and dipyrazolotriazines as promising tyrosyl-TRNA synthetase and peroxiredoxin-5 inhibitors: design, synthesis, molecular docking and structure-activity relationship (SAR) analysis. *Bioorg. Chem.* **2021**, *109*, 104704.
38. Al Mousa, A.A.; Abouelela, M.E.; Mansour, A.; Nasr, M.; Ali, Y.H.; Al Ghamidi, N.S.; Abo-Dahab, Y.; Mohamed, H.; Abo-Dahab, N.F.; Hassane, A.M.A. Wound healing, metabolite profiling, and in silico studies of *Aspergillus Terreus*. *Curr. Issues Mol. Biol.* **2024**, *46*, 11681-11699.
39. Sheibani, H.; Saheb, V.; Rezaei, M.; Zahedifar, M. Chemosensitive three component reactions of 3-aminopyrazoles, aldehydes and malononitrile: Optimize the structures and compute the energies of possible tautomers. *Lett. Org. Chem.* **2014**, *11*, 126-130.
40. Al Mousa, A.A.; Mohamed, H.; Hassane, A.M.A.; Abo-Dahab, N.F. Antimicrobial and cytotoxic potential of an endophytic fungus *Alternaria tenuissima* AUMC14342 isolated from *Artemisia judaica* L. growing in Saudi Arabia. *J. King Saud Univ.* **2021**, *33*, 101462.
41. Jahangirian, H.; Haron, M.J.; Shah, M.H.; Abdollahi, Y.; Rezayi, M.; Vafaei, N. Well diffusion method for evaluation of antibacterial activity of copper phenyl fatty hydroxamate synthesized from canola and palm kernel oils. *Dig. J. Nanomater. Biostructures* **2013**, *8*, 1263-1270.
42. Brand-Williams, W.; Cuvelier, M.-E.; Berset, C. Use of a free radical method to evaluate antioxidant activity. *LWT-Food Sci. Technol.* **1995**, *28*, 25-30.
43. Morris, G.M.; Huey, R.; Lindstrom, W.; Sanner, M.F.; Belew, R.K.; Goodsell, D.S.; Olson, A.J. AutoDock4 and AutoDockTools4: Automated docking with selective receptor flexibility. *J. Comput. Chem.* **2009**, *30*, 2785-2791.